Transverse Phase Space Diagnostics for the 250 MeV Injector

Bolko Beutner

FELSI Meeting 17.3.2009

Introduction

An reliable beam optics matching and emittance measurement is required for the PSI XFEL project for every day operation.

The goal therefore is a easy-to-use standard tool for routine operation.

Additionally a full reconstruction of Phase Space is required for beam dynamics studies.

In this talk the basic methods and algorithms of optics and emittance measurements are presented.

Basic Measurement Principle

Measurement of spot size with varying phase advance is used to determine beam optics properties:

- Multiknob (Quadscan): one or more quads are used to scan the phase advance

- Multiposition: at least three screens are used in a FODO section

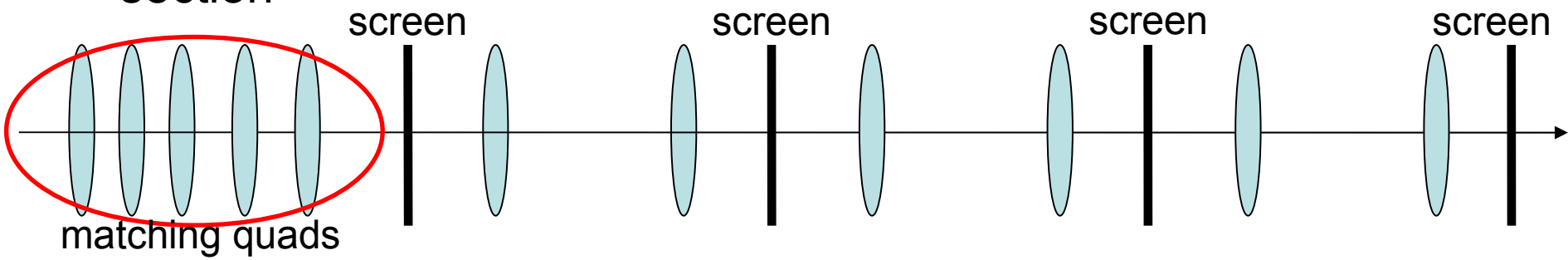

Example: FLASH DBC2

Example:

- FLASH DBC2
- Diagnostic FODO Section
- 45deg phase advance between screens

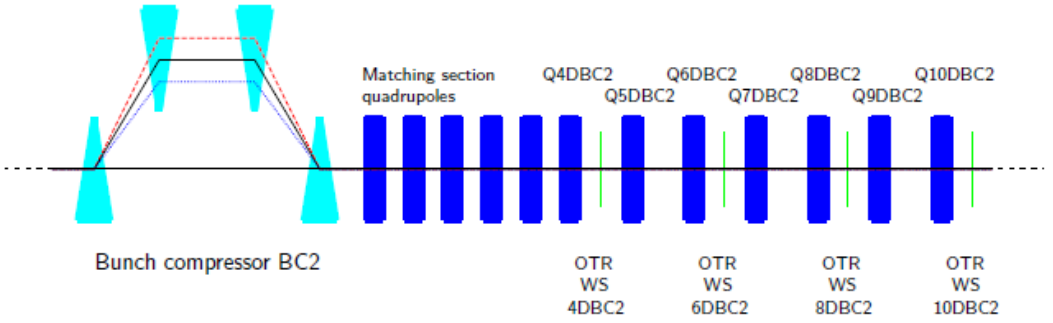

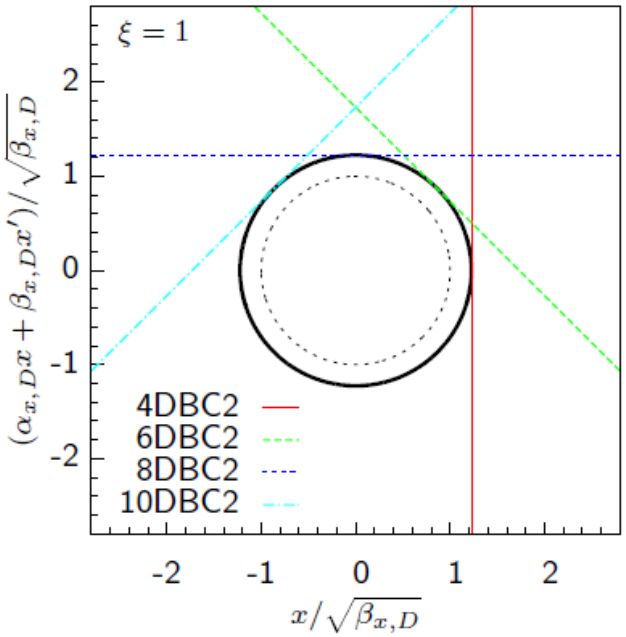

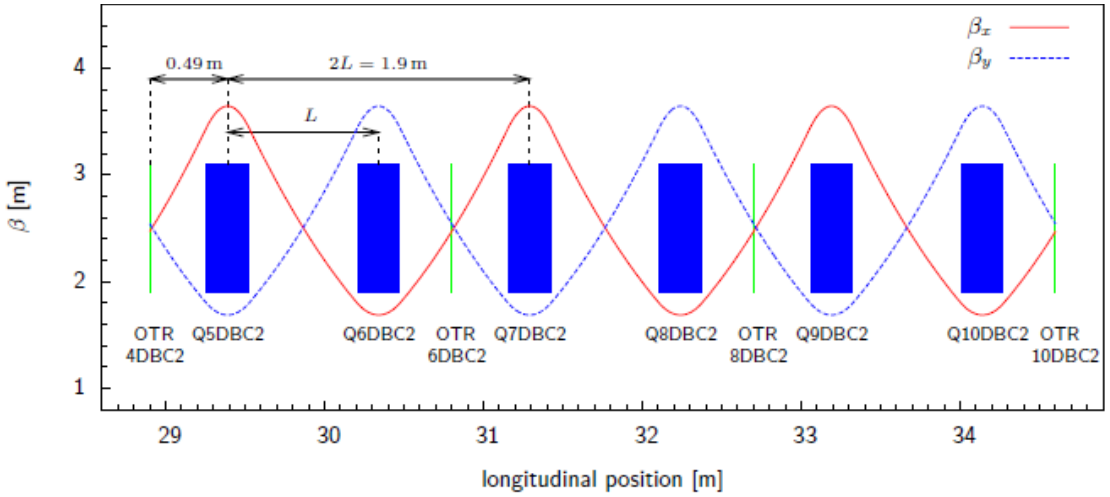

	BC2 (45°)
$\beta_{x,D}$ [m]	2.47
$\alpha_{x,D}$	-1.19
$\beta_{y,D}$ [m]	2.51
$\alpha_{y,D}$	1.21

Florian Löhl

Contents

- RMS Emittance Reconstruction
- Phase Space Tomography
  - Theory
  - MENT: maximum entropy algorithm
- Simulations
- SLS Measurements
- Next steps

RMS Emittance Reconstruction

- Beam spot size for different measurements i = 1,2,3 and corresponding transfer matrices $R^{(i)}$:

$$\begin{pmatrix} \langle x_{(1)}^2 \rangle \\ \langle x_{(2)}^2 \rangle \\ \langle x_{(3)}^2 \rangle \end{pmatrix} = \underbrace{\begin{pmatrix} {R_{11}^{(1)}}^2 & 2R_{11}^{(1)}R_{12}^{(1)} & {R_{12}^{(1)}}^2 \\ {R_{11}^{(2)}}^2 & 2R_{11}^{(2)}R_{12}^{(2)} & {R_{12}^{(2)}}^2 \\ {R_{11}^{(3)}}^2 & 2R_{11}^{(3)}R_{12}^{(3)} & {R_{12}^{(3)}}^2 \end{pmatrix}}_{\boldsymbol{A}} \begin{pmatrix} \langle x_0^2 \rangle \\ \langle x_0 x_0' \rangle \\ \langle {x_0'}^2 \rangle \end{pmatrix}$$

- Matrix inversion: (not optimal for measured data with errors)

$$\begin{pmatrix} \langle x_0^2 \rangle \\ \langle x_0 x_0' \rangle \\ \langle {x_0'}^2 \rangle \end{pmatrix} = \boldsymbol{A}^{-1} \begin{pmatrix} \langle x_{(1)}^2 \rangle \\ \langle x_{(2)}^2 \rangle \\ \langle x_{(3)}^2 \rangle \end{pmatrix}$$

$$\epsilon_{x,\mathrm{rms}} = \sqrt{\langle x_0^2 \rangle \langle {x_0'}^2 \rangle - \langle x_0 x_0' \rangle^2}$$

$$\begin{pmatrix} \beta_{x_0} \\ \alpha_{x_0} \\ \gamma_{x_0} \end{pmatrix} = \begin{pmatrix} \langle x_0^2 \rangle / \epsilon_{x,\mathrm{rms}} \\ -\langle x_0 x_0' \rangle / \epsilon_{x,\mathrm{rms}} \\ \langle {x_0'}^2 \rangle / \epsilon_{x,\mathrm{rms}} \end{pmatrix}$$

- Least squares optimization to measured data with errors:

$$f_i(\langle x_0^2 \rangle, \langle x_0 x_0' \rangle, \langle {x_0'}^2 \rangle) = {R_{11}^{(i)}}^2 \langle x_0^2 \rangle + 2R_{11}^{(i)} R_{12}^{(i)} \langle x_0 x_0' \rangle + {R_{22}^{(i)}}^2 \langle {x_0'}^2 \rangle$$

$$\chi^2 = \sum_{i=1}^{n} \left[\frac{\langle x_{(i)}^2 \rangle - f_i(\langle x_0^2 \rangle, \langle x_0 x_0' \rangle, \langle {x_0'}^2 \rangle)}{\sigma_{\langle x_{(i)}^2 \rangle}} \right]^2$$

Florian Löhl

Bolko Beutner

RMS Emittance Reconstruction

with

$$B = \begin{pmatrix} \frac{R_{11}^{(1)2}}{\sigma_{\langle x_{(1)}^2 \rangle}} & \frac{2R_{11}^{(1)}R_{12}^{(1)}}{\sigma_{\langle x_{(1)}^2 \rangle}} & \frac{R_{12}^{(1)2}}{\sigma_{\langle x_{(1)}^2 \rangle}} \\ \frac{R_{11}^{(2)2}}{\sigma_{\langle x_{(2)}^2 \rangle}} & \frac{2R_{11}^{(2)}R_{12}^{(2)}}{\sigma_{\langle x_{(2)}^2 \rangle}} & \frac{R_{12}^{(2)2}}{\sigma_{\langle x_{(2)}^2 \rangle}} \\ \vdots & \vdots & \vdots \\ \frac{R_{11}^{(n)2}}{\sigma_{\langle x_{(n)}^2 \rangle}} & \frac{2R_{11}^{(n)}R_{12}^{(n)}}{\sigma_{\langle x_{(n)}^2 \rangle}} & \frac{R_{12}^{(n)2}}{\sigma_{\langle x_{(n)}^2 \rangle}} \end{pmatrix} \quad a = \begin{pmatrix} \langle x_0^2 \rangle \\ \langle x_0 x_0' \rangle \\ \langle x_0'^2 \rangle \end{pmatrix} \quad \text{and} \quad b = \begin{pmatrix} \frac{\langle x_{(1)}^2 \rangle}{\sigma_{\langle x_{(1)}^2 \rangle}} \\ \frac{\langle x_{(2)}^2 \rangle}{\sigma_{\langle x_{(2)}^2 \rangle}} \\ \vdots \\ \frac{\langle x_{(n)}^2 \rangle}{\sigma_{\langle x_{(n)}^2 \rangle}} \end{pmatrix}$$

one can express the fit optimisation of

$$\chi^2 = \sum_{i=1}^{n} \left[b_i - \sum_{j=1}^{3} B_{ij} a_j \right]^2$$

with the matrix equation: $a = \left(B^T B\right)^{-1} B^T b$

Numerically this can be more efficient than the fit itself.

Florian Löhl

RMS Emittance Reconstruction

RMS emittance error obtained by error propagation can be expressed in two equivalent formulations.

In computer codes it is often more practical to use Eq. B) for the error calculation.

A)

$$\sigma_g^2 = \sum_{i=1}^{n} \left(\frac{\partial g}{\partial x_i} \right)^2 \sigma_{x_i}^2 + \sum_{i=1}^{n} \sum_{j=1, j \neq i}^{n} \frac{\partial g}{\partial x_i} \frac{\partial g}{\partial x_j} \mathrm{cov}(i,j)$$

$$\boldsymbol{f} = \begin{pmatrix} \beta_{x_0} \\ \alpha_{x_0} \\ \epsilon_{x_{0,\mathrm{rms}}} \end{pmatrix} = \begin{pmatrix} a_1 / \sqrt{a_1 a_3 - a_2^2} \\ -a_2 \sqrt{a_1 a_3 - a_2^2} \\ \sqrt{a_1 a_3 - a_2^2} \end{pmatrix}$$

$$\sigma_{a_k}^2 = \sum_{i=1}^{n} \left(\frac{\partial a_k}{\partial \langle x_{(i)}^2 \rangle} \right)^2 \sigma_{\langle x_{(i)}^2 \rangle}^2$$

B)

$$\sigma_f^2 = (\nabla_a \boldsymbol{f})^T C (\nabla_a \boldsymbol{f}) = \begin{pmatrix} \sigma_{\beta_{x_0}}^2 & \cdots & \cdots \\ \cdots & \sigma_{\alpha_{x_0}}^2 & \cdots \\ \cdots & \cdots & \sigma_{\epsilon_{x_{0,rms}}}^2 \end{pmatrix}$$

M. Minty and F. Zimmermann, *Measurements and control of charged particle beams*, Springer, Berlin, Heidelberg, New York, 2003.

Tomographie

Topographic techniques allow the reconstruction of 2D function values f(x,y) from a set of line integrals trough the point (x,y).

The Radon Theorem guarantees an unique solution for f(x,y) for a suitable set of projections.

Mostly rotations are used to obtain different projections but the theory holds for general linear transformations

=> **Phase Space Reconstruction**.

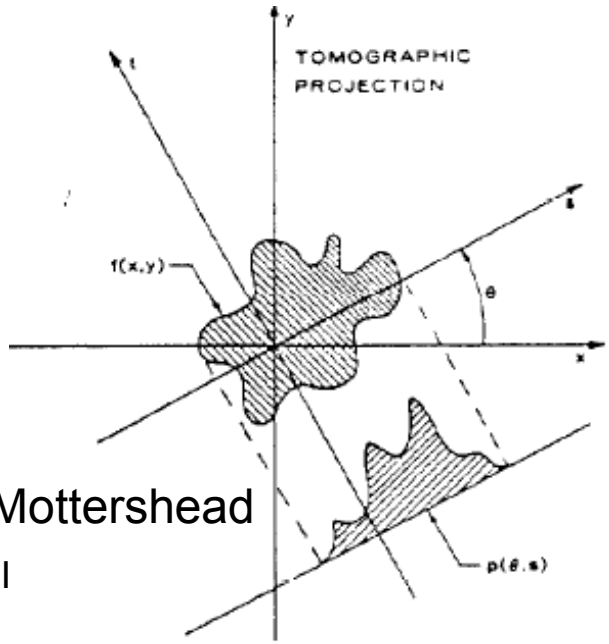

SITZUNG VOM 30. APRIL 1917.

Über die Bestimmung von Funktionen durch ihre Integralwerte längs gewisser Mannigfaltigkeiten.

Von

JOHANN RADON.

Integriert man eine geeigneten Regularitätsbedingungen unterworfene Funktion zweier Veränderlichen x, y — eine *Punktfunktion* $f(P)$ in der Ebene — längs einer beliebigen Geraden g, so erhält man in den Integralwerten $F(g)$ eine *Geradenfunktion*. Das in Abschnitt A vorliegender Abhandlung gelöste Problem ist die Umkehrung dieser linearen Funktionaltransformation, d. h. es werden folgende Fragen beantwortet: kann jede, geeigneten Regularitätsbedingungen genügende Geradenfunktion auf diese Weise entstanden gedacht werden? Wenn ja, ist dann f durch F eindeutig bestimmt und wie kann es ermittelt werden?

Radon Transform

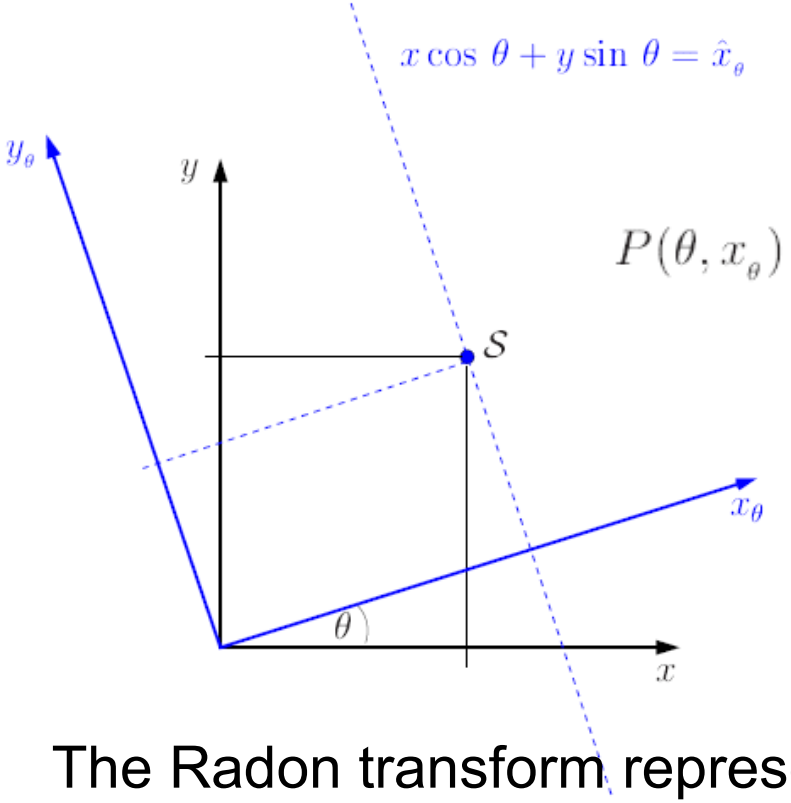

The Radon transform of a 2D-function is given by

$$P(\theta, x_\theta) = \int_{x\cos\theta + y\sin\theta = x_\theta} \rho_{\mathrm{ini}}(x, y)\; dy_\theta$$

$$= \int_{-\infty}^{\infty} \rho_{\mathrm{ini}}(x_\theta \cos\theta - y_\theta \sin\theta\,,\; x_\theta \sin\theta + y_\theta \cos\theta)\; dy_\theta$$

The Radon transform represents the projection along a line trough a point S under a given angle.

In the following introduction I will restrict myself to rotations but general linear maps are possible.

Radon Theorem

From the Fourier transform of the Radon Transform

$$\widehat{P}(\theta,\omega) = \int_{-\infty}^{\infty} P(\theta, x_\theta)\, e^{(-2\pi i\,\omega\, x_\theta)} dx_\theta$$

$$= \int_{-\infty}^{\infty}\int_{-\infty}^{\infty} \rho(x_\theta\cos\theta - y_\theta\sin\theta\,,\; x_\theta\sin\theta + y_\theta\cos\theta)\; e^{(-2\pi i\,\omega\, x_\theta)}\; dx_\theta\, dy_\theta$$

$$= \mathcal{F}(\omega\cos\theta,\; \omega\sin\theta)$$

one can obtain the inverse Radon Transform:

$$\rho(x,\,y) = \int_{-\infty}^{\infty}\int_{-\infty}^{\infty} \mathcal{F}(u,v)\, e^{(+2\pi i\,(x\cdot u + y\cdot v))}\; du\, dv$$

$$= \int_{0}^{\pi}\int_{-\infty}^{\infty} \mathcal{F}(\omega\cos\theta, \omega\sin\theta)\; e^{(+2\pi i\,(x\omega\cos\theta + y\omega\sin\theta))} \begin{vmatrix} \frac{\partial u}{\partial\theta} & \frac{\partial v}{\partial\theta} \\ \frac{\partial u}{\partial\omega} & \frac{\partial v}{\partial\omega} \end{vmatrix} d\omega\, d\theta$$

The Radon Transform is invertable only if *all* (0-180deg) projections are known with *full* (all real numbers) resolution!

Tomographic Reconstruction

For measurements only a finite number of projections is known and with a limited resolution.

The inversion is not possible, but approximate solutions are possible.

In medicine the *filtered back-projection* method is used as a standard approximation.
The profiles are smeared along the projection lines.
Thus a point like object is reconstructed as a star like object.

A spatial high-pass filter is used to correct for this. But a high number of projections is required to get reasonable results.

Filtered Back-Projection

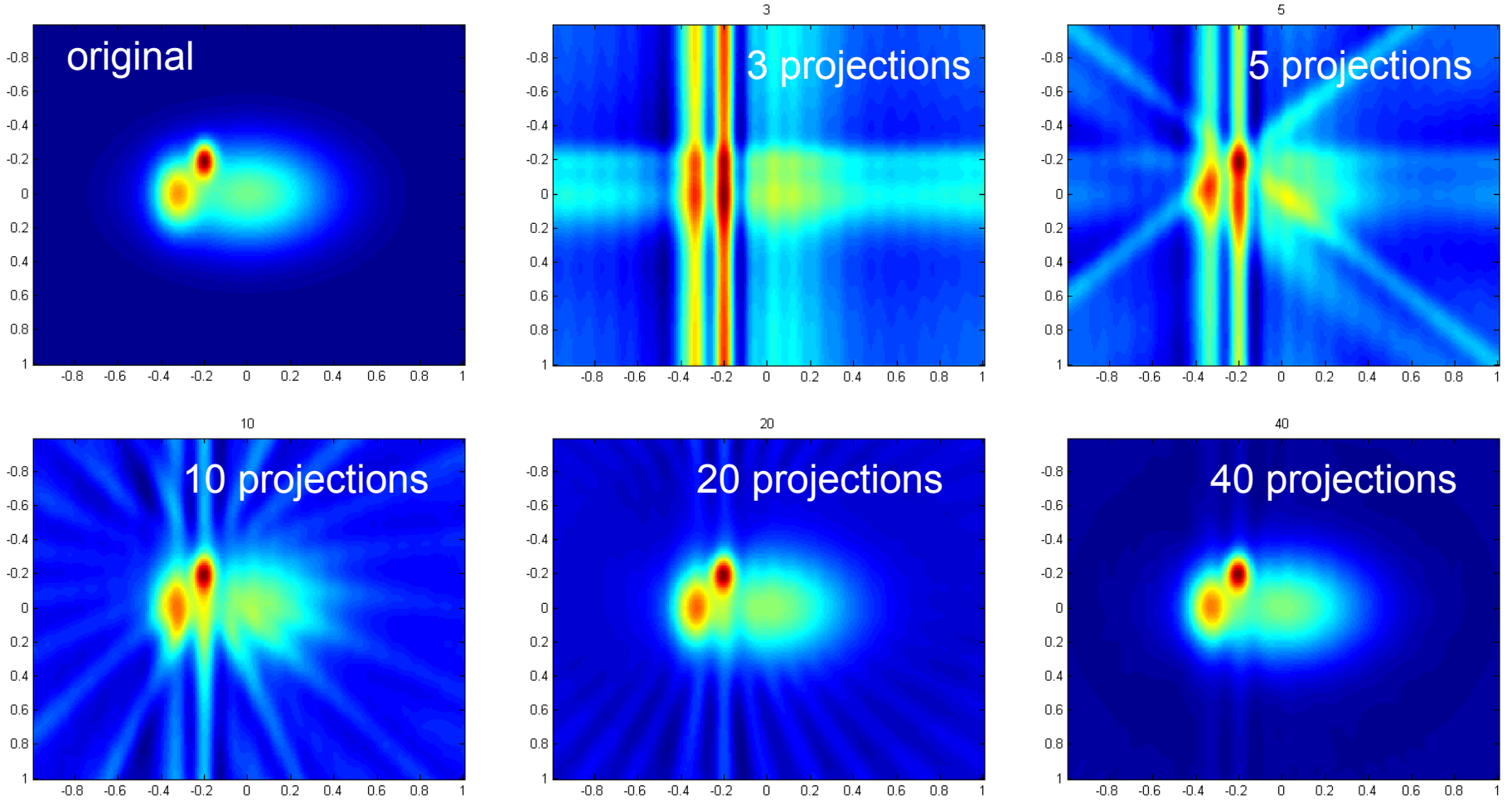

A reasonable reconstruction is only possible for high number of projections. Only if the whole 0-180 deg range is covered in favorable equidistant steps a good reconstruction is possible.

MENT Introduction

For beam diagnostic purposes the *filtered back-projection* is not perfectly suitable, since the phase advance can not set to arbitrary values. In general a 0-180 deg coverage is not possible. A more suitable approach is the *maximum entropy algorithm* (MENT).

Electron beams have little sharp features. This can be formulated by assuming that the electron arrange themselves in the most probable configuration.

=> Entropy is maximised

If one enforces maximum entropy as a general ansatz for the reconstruction with the measured profiles as boundary conditions one obtains a distribution which has the minimal structure compatible with the used projections.

Entropy

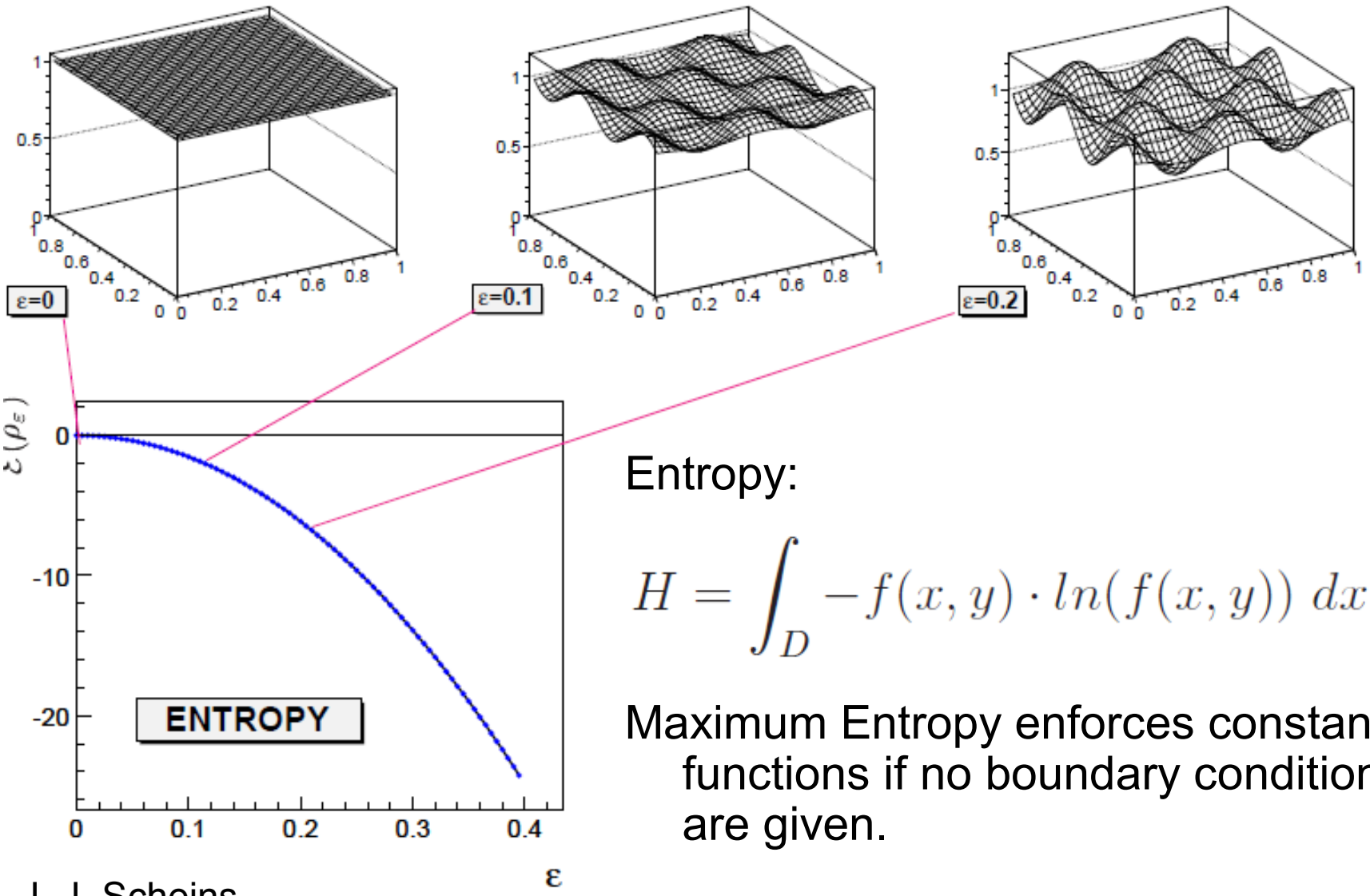

Entropy:

$$H = \int_D -f(x,y) \cdot ln(f(x,y))\ dx\ dy$$

Maximum Entropy enforces constant functions if no boundary conditions are given.

J. J. Scheins

MENT Algorithm

As a consequence the MENT reconstructed function is constant on polygons defined by the projections.

Even for not full equidistant coverage a reconstruction is possible.

J. J. Scheins

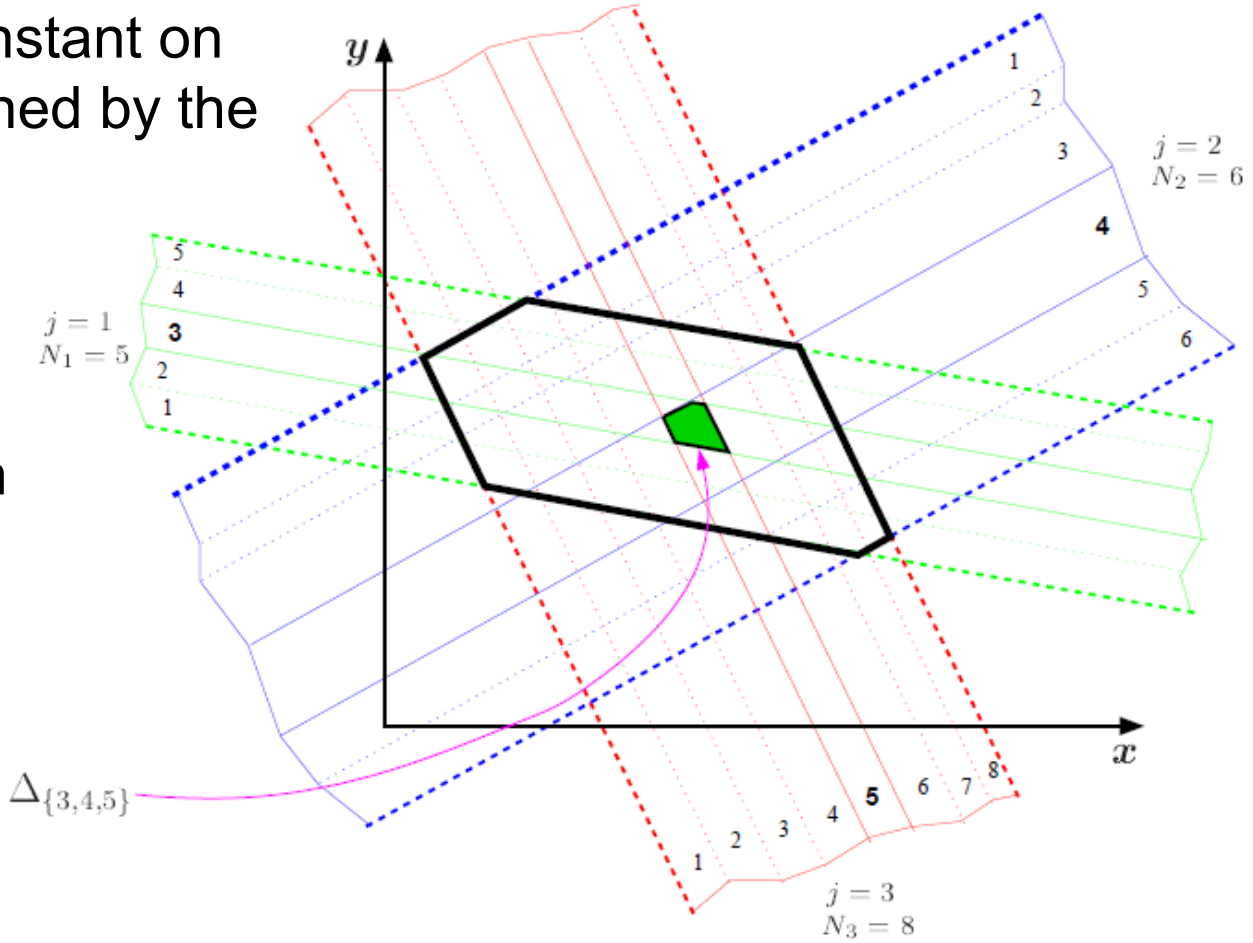

Entropy Optimisation

- Projected Profiles:
  (i)th –projection

$$G_i(x) = \int_{-\infty}^{\infty} \Psi_0\left(x_0^{(i)}(x,x'), {x_0'}^{(i)}(x,x')\right)\,\mathrm{d}x'$$

- Lagrange Function:

$$L(\Psi_0,\boldsymbol{\Lambda}) = -\int_{-\infty}^{\infty}\int_{-\infty}^{\infty} \Psi_0(x_0,x_0')\ln\Psi_0(x_0,x_0')\,\mathrm{d}x_0\,\mathrm{d}x_0'$$

$$+\sum_{i=1}^{n}\int_{-\infty}^{\infty}\left[\int_{-\infty}^{\infty}\Lambda_i(x)\left(\Psi_0\left(x_0^{(i)}(x,x'),{x_0'}^{(i)}(x,x')\right)\mathrm{d}x' - G_i(x)\right)\right]\mathrm{d}x$$

- Lagrange Equations:

$$\frac{\partial L(\Psi,\boldsymbol{\Lambda})}{\partial\Psi} = 0$$

$$\frac{\partial L(\Psi,\boldsymbol{\Lambda})}{\partial\Lambda_i} = 0$$

G. N. Minerbo, *MENT: A Maximum Entropy Algorithm for reconstructing a source from projection data*, Comp. Graphics Image Proc. 48 (1979).

- Solution:

$$\Psi_0(x_0,x_0') = \exp\left[\sum_{i=1}^{n}\Lambda_i\left(x^{(i)}(x_0,x_0')\right) - 1\right]$$

Determination of Lagrange Multipliers

The Lagrange Multipliers can be rewritten as H.

Multiplication of these Factors give then the phase space distribution.

$$H_i(x) = \exp\left[\Lambda_i(x) - \frac{1}{n}\right]$$

$$\Psi_0(x_0, x_0') = \prod_{i=1}^{n} H_i\left(x^{(i)}(x_0, x_0')\right)$$

Plugging this in the definition leads after factorisation to a iteration law for H_i. This can be determined, for example, by a non-linear Gauss-Seidel algorithm.

$$G_i(x) = \int_{-\infty}^{\infty} \prod_{j=1}^{n} H_j\left(x^{(j)}(x_0^{(i)}, x_0'^{(i)})\right) \mathrm{d}x'$$

$$G_i(x) = H_i(x) \int_{-\infty}^{\infty} \prod_{j\neq i}^{n} H_j\left(x^{(j)}(x_0^{(i)}, x_0'^{(i)})\right) \mathrm{d}x'$$

MENT Test

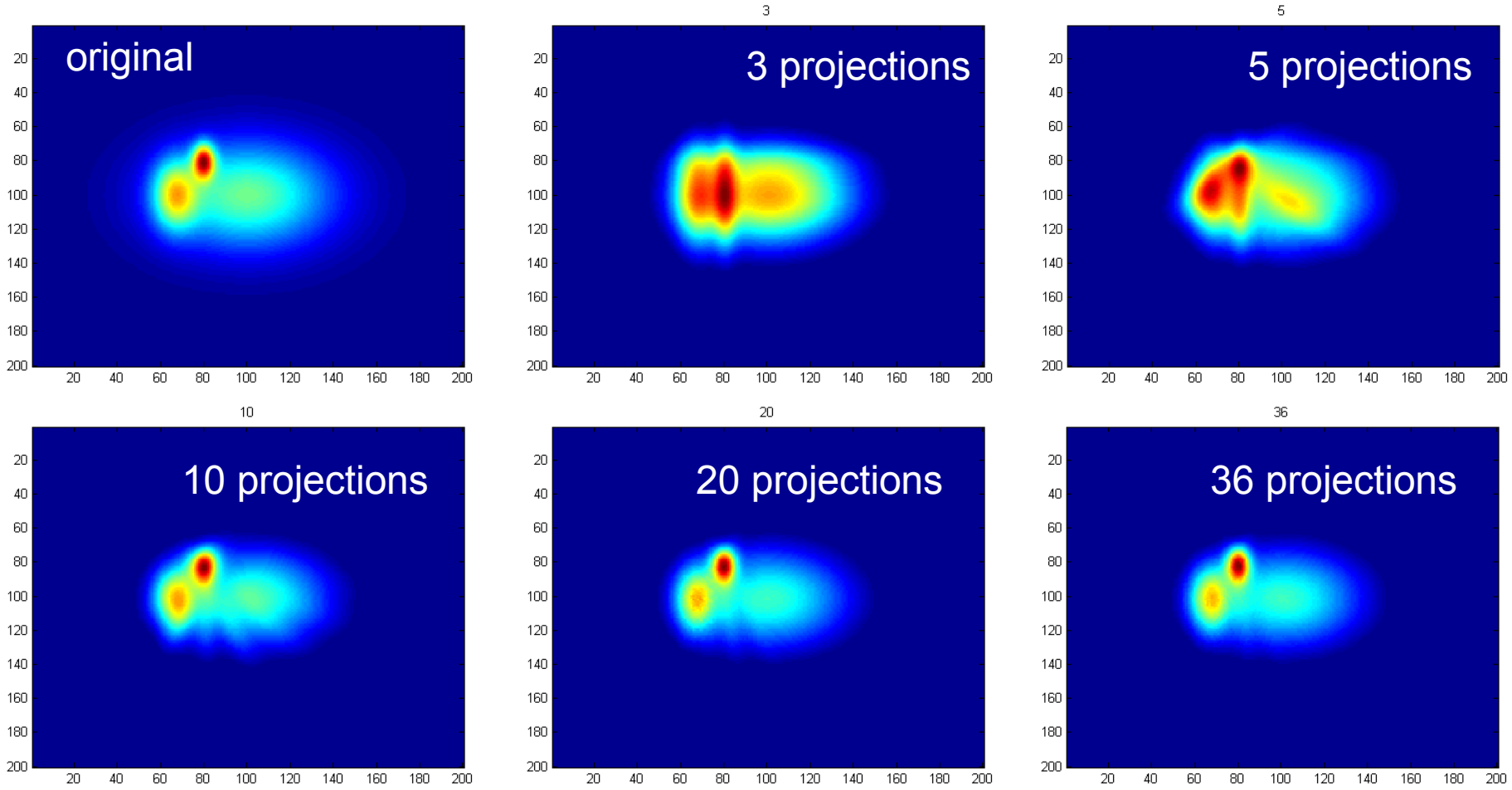

A good reconstruction requires only an small number of projections.

40 iterations

Summary of the Tests

- Image comparison:

$$\delta_{rec} = \sqrt{\frac{\int_{-\infty}^{\infty}\int_{-\infty}^{\infty} [\Psi_{rec}(x,x') - \Psi_0(x,x')]^2 \, \mathrm{d}x \, \mathrm{d}x'}{\int_{-\infty}^{\infty}\int_{-\infty}^{\infty} [\Psi_{rec}(x,x')]^2 \, \mathrm{d}x \, \mathrm{d}x'}}$$

Especially for low number of projections the *MENT algorithm* gives better results than the *filtered back-projection*.

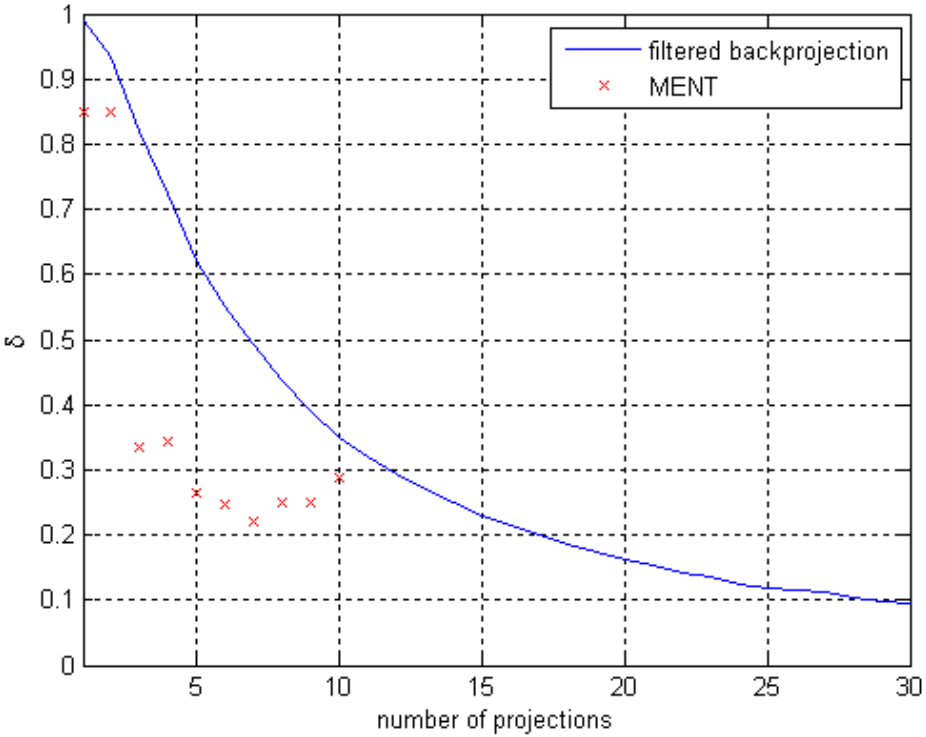

Emittance Reconstruction Simulation

- Simulations done with transport matrices from initial phase space ellipse. Emittance is set to 100mm mrad normalized (100MeV).
- Beam sizes are assumed to have an error of 1%.

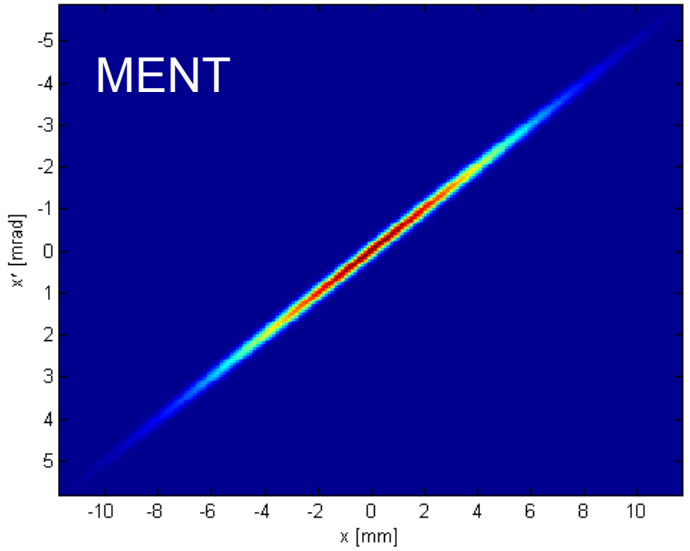

	original	fit	matrix inversion	Error from matrix inv.	MENT
Geo. Emitt.	5.110e-007	5.107e-007	5.108e-007	3.512e-009	5.193e-007
Beta	30.00	29.80	29.80	3.275e-001	29.68
Alpha	15.00	14.90	14.90	1.630e-001	14.84
Gamma	7.533	7.486	7.486	-	7.454

First Results from the SLS Linac

- SLS LINAC

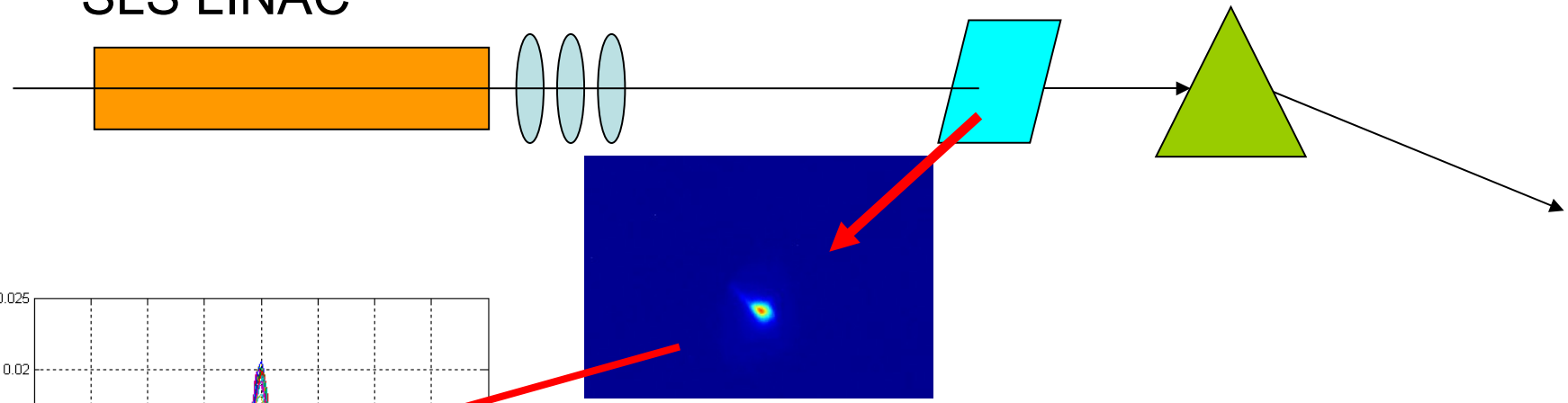

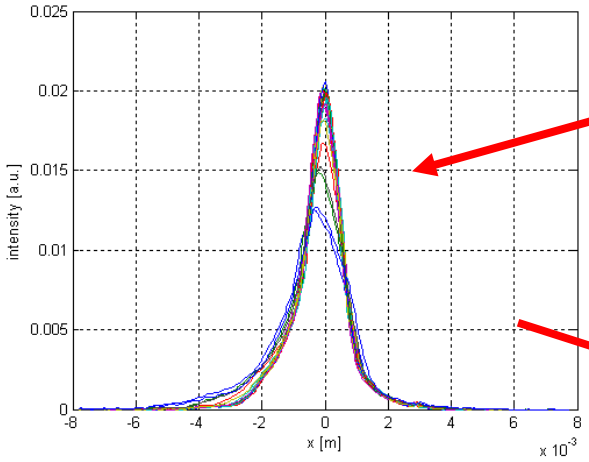

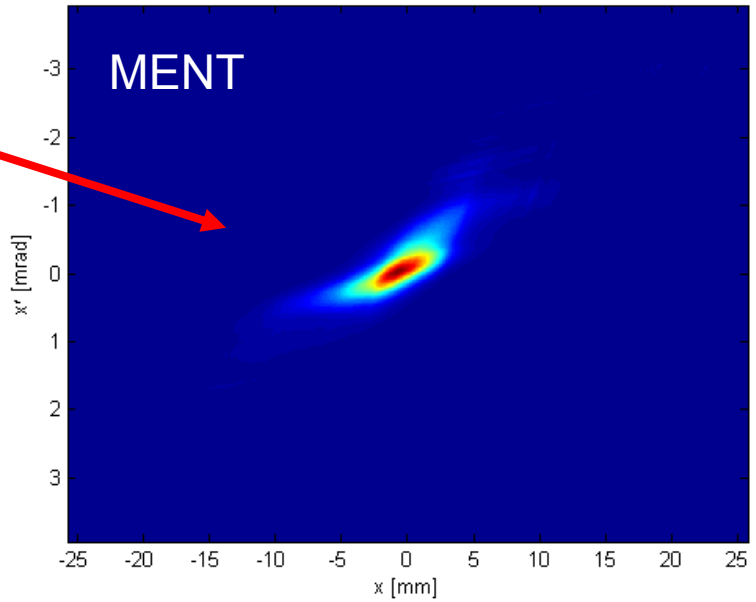

Preliminary Results

First measurements on the SLS linac with a new digital camera.

MENT reconstruction was done quick-and-dirty. Especially the image post processing has to be improved to mitigate noise which degrades the reconstruction.

Slightly different transfer matrices models were used.

Spot size was not optimal during the measurements
=> limited resolution

	SLS standard monitor	XFEL experimental setup	MENT (90%)
Beta [m]	7.03	8.70	12.5906
Alpha [rad]	-0.77	0.35	1.3472
Geo. Emitt. [umrad]	0.34	0.42	0.36

Next Steps

- Improvement of Image post Processing for MENT reconstruction - further analysis of SLS Linac Data
- Studies on systematic errors in the 250MeV diagnostic section and the PSI-XFEL (Simulations)
  - Energy Errors (Mismatch in FODO-Section)
  - Space Charge Effects

- Development of an stable Operation Tool for emittance measurement and optics matching
- Adaption of these techniques to slice emittance analysis with a transverse deflecting RF structure

Thank You
for Your
Attention!

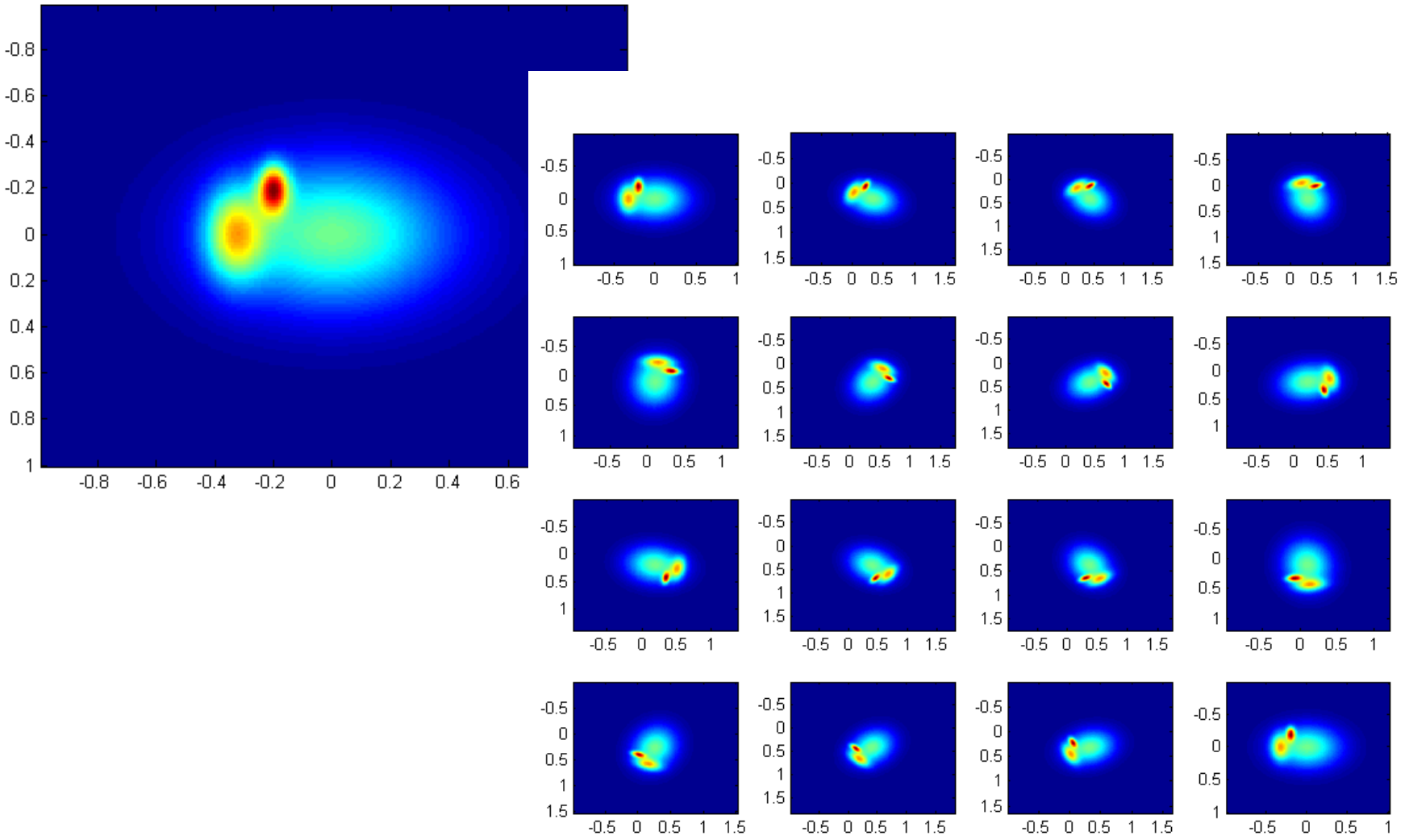
-0.8
-0.6
-0.4
-0.2
0
0.2
0.4
0.6
0.8
1
-0.8 -0.6 -0.4 -0.2 0 0.2 0.4 0.6
-0.5 0 0.5 1
-0.5 0 0.5 1 1.5

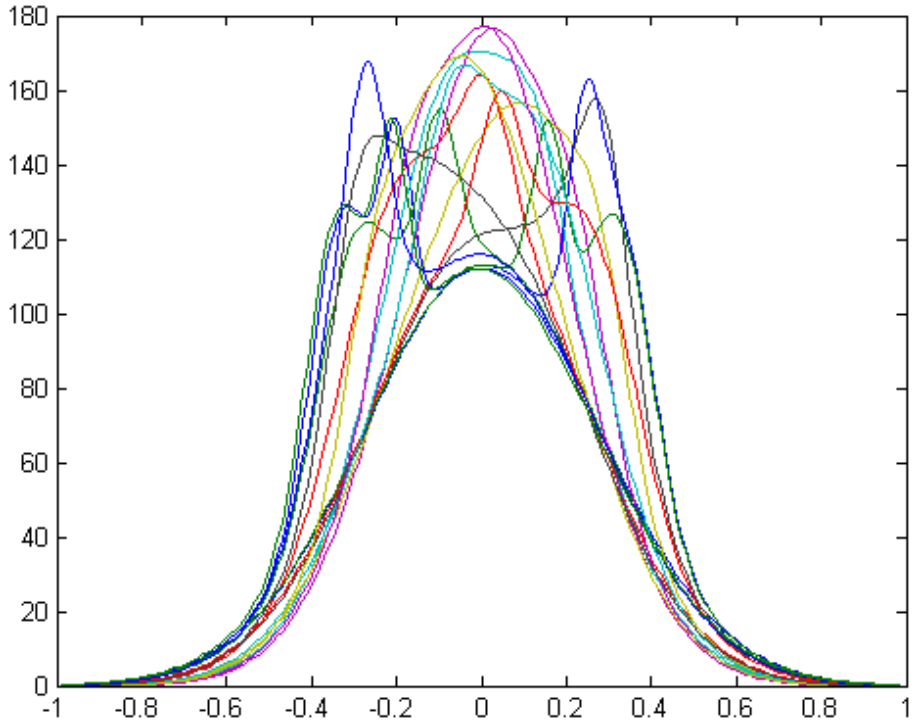
180
160
140
120
100
80
60
40
20
0
-1
-0.8
-0.6
-0.4
-0.2
0
0.2
0.4
0.6
0.8
1

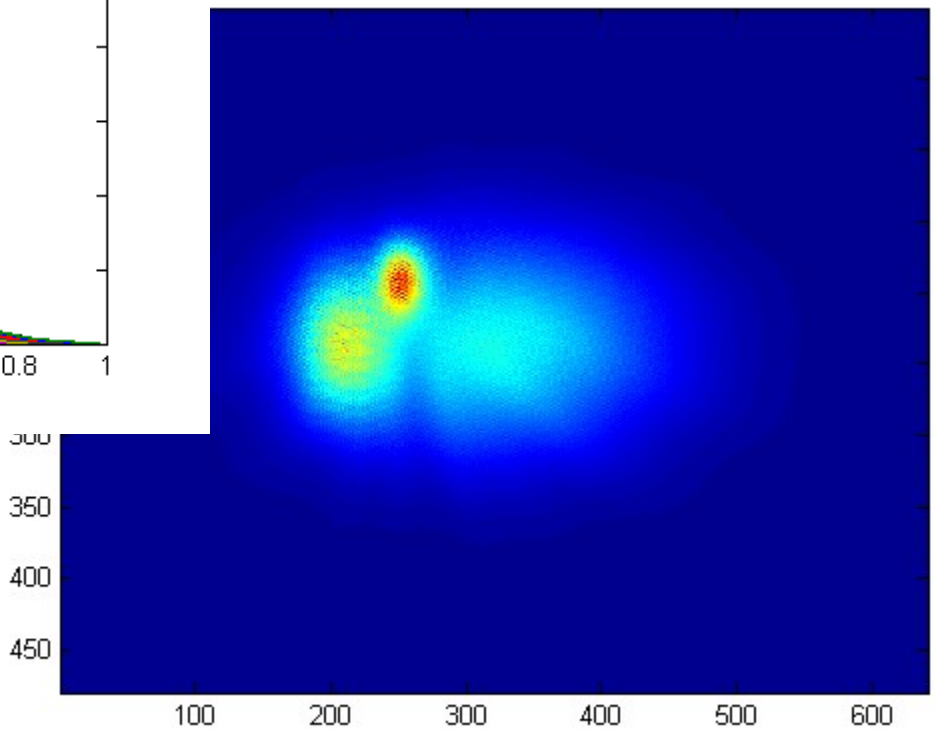
350
400
450
100
200
300
400
500
600

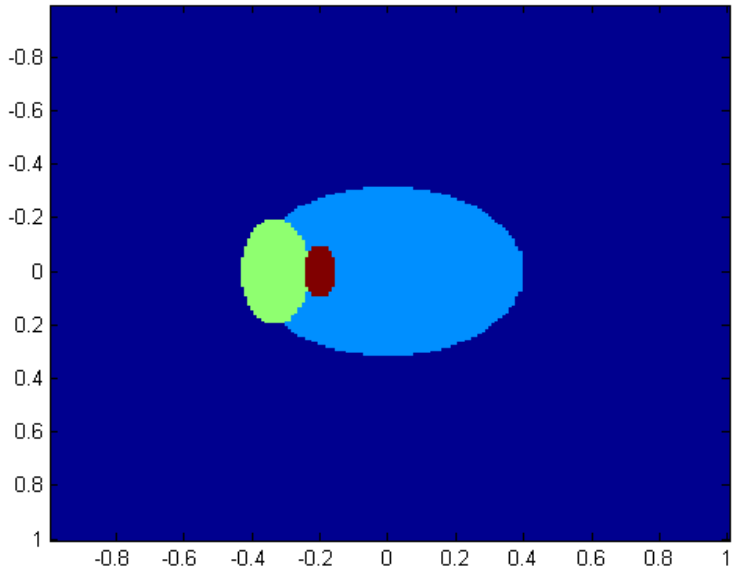
-0.8
-0.6
-0.4
-0.2
0
0.2
0.4
0.6
0.8
1
-0.8
-0.6
-0.4
-0.2
0
0.2
0.4
0.6
0.8
1

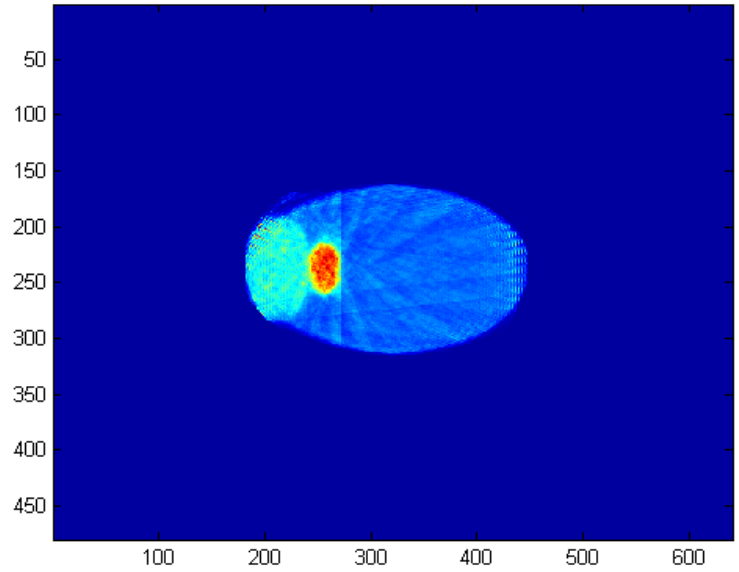
50
100
150
200
250
300
350
400
450
100
200
300
400
500
600